Processing and Application of Ceramics 19 [4] (2025) 408–417
https://doi.org/10.2298/PAC2504408D

Effect of Vickers indentation defects on the biaxial flexural strength of float glass in wet environments: A Weibull analysis

Oualid Dairi[1,*], Mohamed Hamidouche[1], Zahra Malou Hamidouche[1], Mohamed Ilyes Habia[2], Tarek Bali[1], Akram Zegadi[1], Mohamed Liamine Bella[1]

[1]*Emerging Materials Research Unit, University of Setif 1, Algeria*
[2]*Applied Optics Laboratory ,University Setif 1, Algeria*

Received 12 July 2025; Received in revised form 9 December 2025; Accepted 19 December 2025

Abstract

This research examines how Vickers indentation-induced flaws affect the strength and failure probability of Mediterranean float glass (MFG), specifically under biaxial flexural testing in distilled water. In total, fifteen square samples (50 × 50 mm^2 each) were subjected to a constant loading rate of 0.3 mm/min. Controlled defects were introduced using loads of 1 and 10 N at three distinct distances from the high-stress contact point (2, 10 and 18 mm) of the ring-on-ring bending device. The Weibull statistical distribution was utilized to capture the relationship between defect characteristics and the glass's mechanical behaviour. Key findings indicate that higher indentation loads (10 N) produce more severe flaws, which consistently lower both the mean time to failure (MTTF) and the Weibull scale parameter (η), regardless of flaw position. Defects placed closer to the region of maximum stress, i.e. near the contact area, create stronger stress concentrations and thus a notable reduction in fracture resistance. The presence of water further aggravates these effects by accelerating crack growth, increasing stress concentrations and ultimately undermining the mechanical integrity of the glass. Analysis of the Weibull parameters revealed that the shape parameter (β) decreases as flaws approach the high-stress region, suggesting greater heterogeneity and criticality of defects. The scale parameter (η) also varies with both indentation load and defect location, underlining the inherent variability in glass strength depending on these factors. These results emphasize the need to account for both flaw geometry and environmental influences such as humidity when designing and applying float glass materials.

Keywords: *float glass, ring-on-ring test, strength, water, defects*

I. Introduction

Despite its widespread use in architectural, automotive and industrial applications, the mechanical performance of float glass remains highly sensitive to surface defects and environmental conditions. Surface defects in float glass are a major concern for quality control and safety. Various methods have been developed to detect and characterize these defects. Thus, Fourier ptychographic microscopy and microfractographic analysis enable glass surface defects to be detected, counted and measured, providing quantitative data on parameters such as length, width, orientation and depth [1,2]. The fringe projection digital profilometer offers an online defect detection method for float glass, using phase information to identify and reconstruct surface defects, thus achieving high detection accuracy of optical distortion defects [3].

Numerous studies have highlighted the crucial role of defects such as microcracks, surface flaws and abrasions in determining the strength and fracture behaviour of glass elements under different loading conditions. The presence, size, orientation and distribution of defects, such as microcracks, have been linked to the macroscopic strength of float glass, influencing its fracture toughness [4,5]. In addition, the influence of defect characteristics, such as size and shape, on glass strength has been assessed by means of biaxial testing, providing information on fracture mechanics and structural strength assessment [6].

Defects in glass and glass-ceramic materials have a significant impact on the Weibull parameters, which are

*Corresponding author: +213771024448
e-mail: *walid_opt04@yahoo.fr*

essential for understanding the variability of material strength [7,8]. The presence of microcracks, edge defects and internal flaws leads to scattered test results, necessitating the use of probabilistic failure criteria such as the Weibull distribution [9]. Recent advances in fracture mechanics have highlighted the importance of considering stress concentration effects and environmental factors in the assessment of brittle material failure [10,11].

Water has a significant impact on the mechanical properties of glass-based materials. Studies have shown that water absorption affects the mechanical properties of composites, such as tensile and flexural strengths, by modifying their water-ageing behaviour [12]. The presence of water molecules on glass surfaces can influence various properties such as adhesion, stress corrosion, indentation, scratching, and wear behaviour, ultimately affecting the mechanical and mechanochemical properties of glass [13]. Furthermore, it has been shown that the ageing of fibre-reinforced polymer composites in different types of water (tap, sea, rain) reduces the tensile and flexural strengths of glass fibre-epoxy composites, with some recovery in strength observed after re-drying the samples [14]. The Weibull parameters of glass and ceramics are also affected by environmental conditions, showing variations in microhardness values depending on the liquid used [15].

Richardson *et al.* [16] showed that the presence of water in float glass has an impact on the Weibull parameters, in particular the Weibull modulus. They demonstrated that the kinetic brittleness of soda-lime-silica glasses decreases with hydration, even if water dissolves in the glasses in the form of OH groups, which could depolymerize the network.

However, despite these studies, there is a lack of comprehensive research on how Vickers indentation-induced defects affect the biaxial flexural strength of float glass in wet environments. Most existing studies focus on general defect characterization or the effects of water on mechanical properties without considering the specific interaction between indentation-generated defects and the mechanical response of glass under humid conditions. This gap in the literature highlights the need for a more targeted study to address the following question: How do indentation-induced defects influence the biaxial flexural strength of float glass in the presence of water?

The aim of this study is to evaluate the resistance of samples to biaxial ring-on-ring bending in the presence of water, by studying the defects caused by Vickers indentation at various distances from the contact point. The main objective is to understand the reaction of samples to fracture or deformation under specific loads, considering the effect of the aqueous environment. The study also aims to analyse the distribution of defects using the statistical Weibull distribution, to model how the probability of failure evolves as a function of distance from the contact point, applied load, and the presence of water.

II. Experimental

2.1. Weibull analysis

The Weibull distribution is a powerful tool widely used in reliability engineering and materials science. It provides information on product reliability, failure rates and lifetime predictions [17,18]. Mathematical models of the distribution, such as Weibull mixtures, are essential for understanding complex data sets with distinct fault distributions and failure mechanisms [19]. Derivation of the Weibull parameters from mechanical strength measurements is essential for predicting the service life of stressed materials, enabling maintenance and replacement intervals to be optimized [20].

Statistical distributions of fracture-related mechanical properties, such as fracture stress, elongation, fracture toughness and fatigue life, can be related to the distribution of defects. Statistically, this implies that the worst (largest) defect is the one that determines the mechanical properties related to the fracture, thus constituting the "weakest link". Based on the "weakest link" theory, Weibull [21] introduced an empirical distribution that has since been widely used for ceramics and metals. The cumulative probability function of the Weibull distribution is expressed as [22]:

$$P = 1 - \exp\left[-\left(\frac{\sigma - \sigma_T}{\eta}\right)^{\beta}\right] \tag{1}$$

where P is the probability of failure at a given stress σ or below. The threshold value σ_T is the value below which no sample is likely to fail. The term η is the scaling parameter, and β is the shape parameter, also known as the Weibull modulus. One of the most commonly used methods for presenting Weibull fits to data is the Weibull probability plot. After rearrangement, Eq. 1 can be written as [23]:

$$\ln[-\ln(1 - P)] = \beta \ln(\sigma - \sigma_T) - \beta \ln(\eta) \tag{2}$$

Note that Eq. 2 has a linear form when the left-hand side of the equation is plotted as a function of $\ln(\sigma - \sigma_T)$ with a slope of β and a y-intercept of $-\beta \cdot \ln(\eta)$. This method of presentation gives a linear relationship only when $\sigma_T = 0$.

The Weibull modulus β is a material parameter that characterizes defect dispersion, and it characterizes the width or range of the defect size distribution. A high value of β corresponds to a population of defects with uniform sizes, while a low value indicates greater variability in defect characteristics. The probability P_i is defined by [24]:

$$P_i = \frac{i}{N + 1} \tag{3}$$

where i represents the rank of each measured value after ordering all values in ascending order and N represents the total number of measurements in the sample under test [25].

In this study, Weibull parameters were estimated using the linear regression method applied to Eq. 2, which is equivalent to the least squares method on the Weibull probability plot. The goodness of fit was assessed using the coefficient of determination (R^2), with all fits yielding $R^2 > 0.95$, indicating excellent agreement between the experimental data and the Weibull model. It is important to acknowledge that the relatively limited sample size (15–30 specimens per condition) may affect the precision of Weibull parameter estimation. However, previous studies have demonstrated that sample sizes in this range can yield sufficiently reliable estimations of the Weibull parameters under conditions of high data quality and rigorously controlled experimental procedures [26,27].

2.2. Investigated glass

The glass material examined in our study comes from Mediterranean float glass (MFG) and is obtained by local float glass manufacturing method with a thickness of 3 mm and dimension of $50 \times 50\,mm^2$. The characteristics and specifications of this material are the following: Poisson's coefficient is 0.22, Young's modulus is 72 GPa, breaking stress is 88 MPa, Vickers hardness is 4.7 GPa, fracture toughness is $0.74\,MPa{\cdot}m^{0.5}$ and density $2.51\,g/cm^3$. Chemical composition data are obtained using the X-ray fluorescence (XRF) method and mass fractions of components are the following: 70.1 wt.% of SiO_2, 14.4 wt.% of Na_2O, 9.12 wt.% of CaO, 0.826 wt.% of MgO, 0.515 wt.% of Al_2O_3, 0.156 wt.% of K_2O and 0.075 wt.% of SO_3.

2.3. Flexural strength testing

An instrumented indentation device, model M30, designed by QNESS and equipped with TX2 software, was used to make indentations. Two separate loads, of 1 and 10 N, were applied to test specimens for 15 s each. These tests involved varying the distance from the centre of the specimen, ranging from 8 to 16 mm from the centre of the specimen, whose dimensions are $50 \times 50\,mm^2$, as shown in Fig. 1. The choice of indentation loads (1 and 10 N) was based on previous studies on Vickers indentation of soda-lime silicate glass, where these forces are known to simulate typical surface flaws such as micro-scratches and lateral cracks, respectively [28,29]. The selected distances (8–16 mm from the centre) correspond to different stress regions under the ring-on-ring bending configuration, allowing for the evaluation of defect sensitivity in relation to maximum tensile stress zones. This range also reflects potential variations in defect positions that may occur during real world handling and installation of float glass panes.

Strength characterization was carried out by concentric biaxial bending tests in a humid environment in the presence of distilled water, as illustrated in Fig. 2. This method offers a significant advantage over three- and four-point devices, as it essentially avoids edge imperfections, thus facilitating the determination of intrinsic strength. For these tests, sets of 30 samples of identical size ($50 \times 50\,mm^2$) were used. It is acknowledged that while the sample size of 15–30 specimens per condition is consistent with previous glass testing studies, larger sample sizes would provide more robust statistical estimates of the Weibull parameters. Nevertheless, rigorous experimental control and high data quality ensure that the obtained parameters provide meaningful insights into the failure behaviour of indented glass under wet conditions.

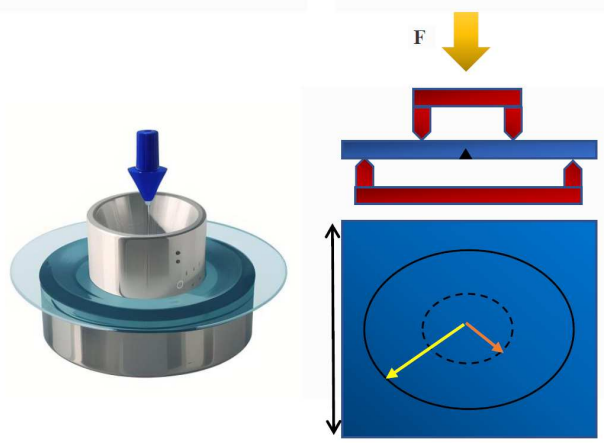

Figure 2. Schematic of concentric biaxial bending test setup: a) cross-sectional view and b) top view showing sample dimensions

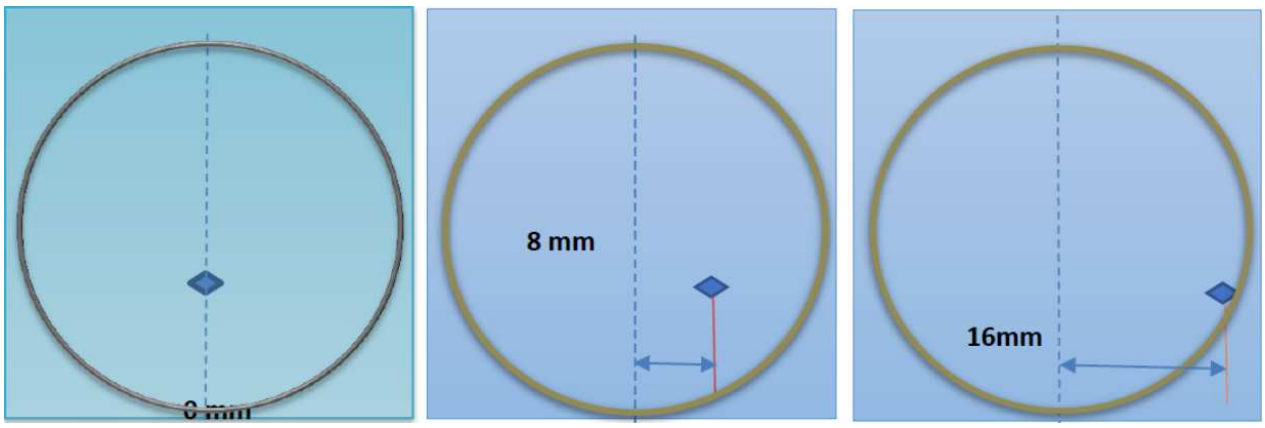

Figure 1. Schematic showing different positions of indentations in relation to the upper ring limit

The device used in this study consists of inner and outer rings with diameters of 16 and 36 mm, respectively. Defects were introduced on the underside, as shown in Fig. 2b. The loading rate was kept constant at 0.3 mm/min for all tests. Stresses at failure (σ) were evaluated according to the relationship [30]:

$$\sigma = \frac{3F_R}{2\pi h^2}\left[(1+\nu)\ln\frac{R_1}{R_2} + (1+\nu)\frac{R_1^2 - R_0^2}{2R_2^2}\right] \quad (4)$$

In this equation, the following variables were used: F_R represents the breaking force and ν is the Poisson's ratio of the glass, set at 0.22. The value of h corresponds to the thickness of the sample, which was set at 3 mm. With regard to the rings radii, R_0 denotes the radius of the inner ring, measured at 8 mm, and R_1 is the radius of the outer ring, measured at 18 mm. The length of the side of the square sample was 50 mm, which corresponds to a value of $2L$, and R_2 was:

$$R_2 = \frac{L(1+\sqrt{2})}{2} \approx 1.21L \quad (5)$$

III. Results

Using two distinct loads (1 and 10 N) placed at three different distances (18, 10 and 2 mm) from the point of contact with the lower ring, Vickers indentation was used to create controlled defects in ring-on-ring bending tests conducted on float glass plates submerged in distilled water. The obtained results are shown in Fig. 3 and Table 1.

The findings revealed that defects made with the highest load (10 N) had significantly lower mean time to failure (MTTF is 30.55 h) and lower scale factor (η = 31.25 MPa) for the furthest defects (18 mm), while defects made with 1 N load had η of 58.03 MPa and MTTF of 53.11 h. In both cases, the shape factor (β) was 4.0. For the closest defects (2 mm), those made with 10 N produced higher MTTF (78.91 h) and η (88.14 MPa) compared to 1 N defects (MTTF was 66.80 h, η = 74.48 MPa). In these circumstances, the β factor was 3.0. The trend was similar for defects at intermediate distance (10 mm), with β factor of 3.0.

Figure 4 presents the median values observed for different test configurations in the ring-on-ring bending test. For a load of 1 N at a distance of 18 mm from the contact point, the median value was 51.81 MPa (Fig. 4). When the load increased to 10 N at the same distance, the median value decreased significantly to 30.56 MPa (–40.9%). The median value increased substantially to 74.41 MPa when the distance was reduced to 2 mm with a load of 10 N (+43.6% relative to baseline). The median value decreased slightly to 63.27 MPa when the distance remained at 2 mm but the load was reduced to 1 N (+22.1% relative to baseline). With a load of 10 N at 10 mm distance, the median value was 45.02 MPa (–13.1%), while at 1 N and 10 mm, it increased slightly to 55.57 MPa (+7.2%).

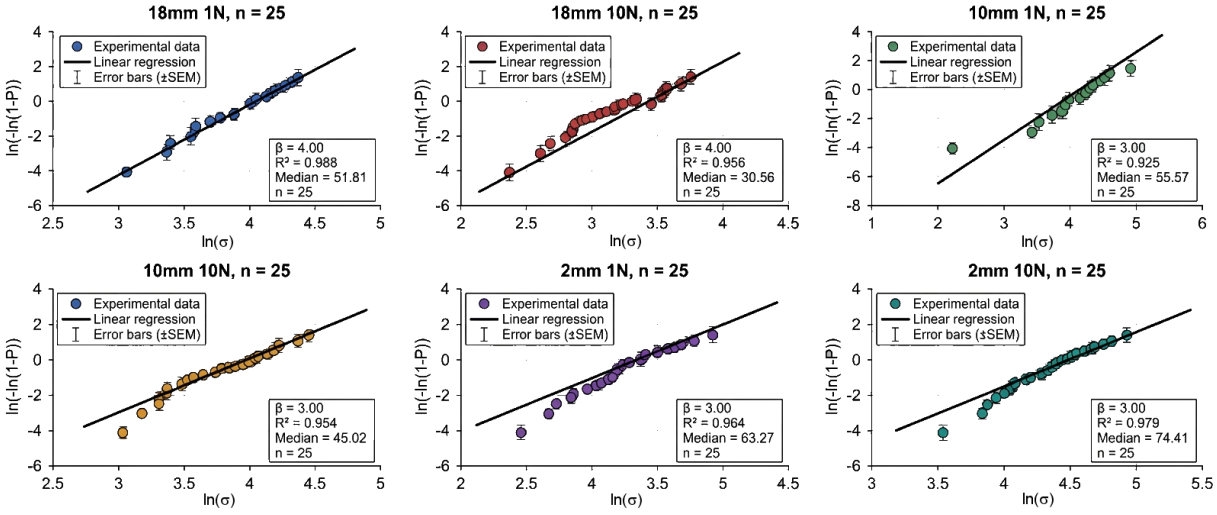

Figure 3. Log-normal distribution for different distances and applied loads (n = 25 samples per configuration), where error bars represent 95% confidence intervals

Table 1. Summary of Weibull parameters (β and η) and mean time to failure (MTTF) for different test configurations

Distance [mm]	Load [N]	β (shape)	η (scale) [MPa]	MTTF [h]	R^2
18	1	4.0	58.03	53.11	0.985
18	10	4.0	31.25	30.55	0.982
10	1	3.0	63.63	57.65	0.978
10	10	3.0	52.86	47.45	0.980
2	1	3.0	74.48	66.80	0.976
2	10	3.0	88.14	78.91	0.979

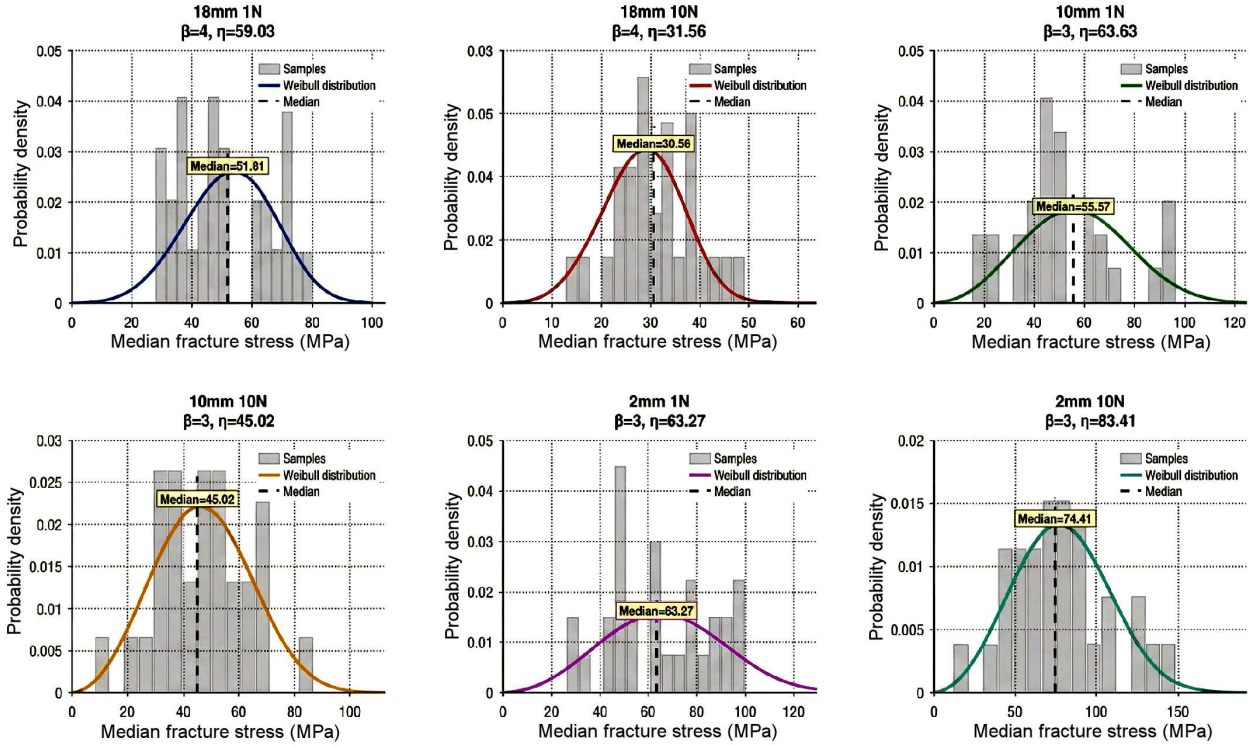

Figure 4. Median values for different parameters (distance *d* and load *P*), where error bars represent standard error (*n* = 25)

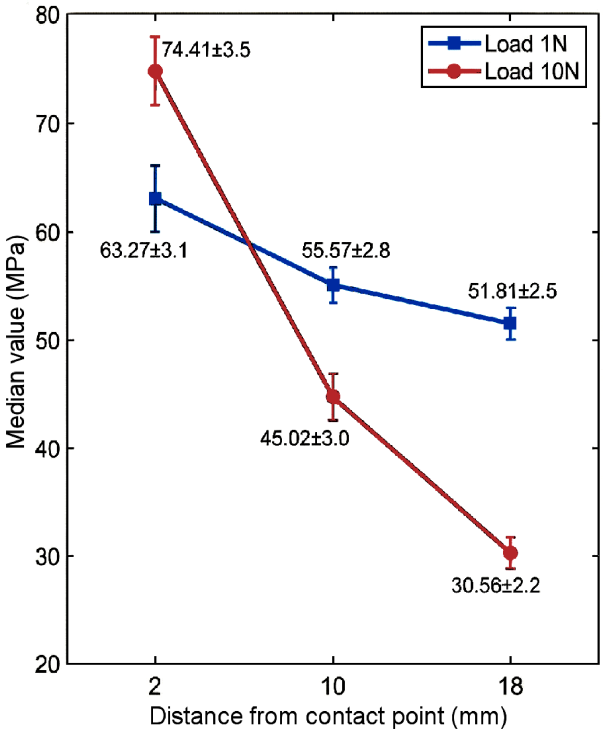

Figure 5. Evolution of median values as a function of indentation defect distance and applied load in ring-on-ring bending tests, blue and red lines correspond to 1 N and 10 N loads, respectively (*n* = 25 per data point)

Changes of the median value with the distance of the defect caused by Vickers indentation for two different loads, 1 and 10 N, are also shown in Fig. 5. The observed trends show that, in general, when the load goes up, the median value decreases. This does not happen only when the distance is close to the contact point, when the median values go up a lot. The results presented in Fig. 5 show that load and distance have a complicated effect on how glass sheets behave when they are pushed down on, with load having the most effect but with big changes depending on where the defects are in relation to the contact point.

Figure 6 shows the cumulative probability of failure as a function of time for ring-on-ring bending tests performed on glass sheets in a water-filled environment. The presence of water can have a significant effect on mechanical behaviour through processes such as stress corrosion cracking. The cumulative probability curves of failure illustrate how the probability of failure evolves over time with different loads (1 and 10 N) and distances from the contact point of the lower ring. Thus, the results in Fig. 6 demonstrate that the increased load generally accelerates crack propagation, which increases the probability of failure rapidly. However, reducing the distance from the contact point significantly improves the resistance to failure, as evidenced by the longer median times for configurations at 2 mm compared to those at 18 mm. This trend demonstrates the importance of test geometry in mitigating the detrimental effects of high loads. Although a higher load consistently accelerates failure, the effect of distance becomes more pronounced at lower loads. It should be added that water can modify the mechanical behaviour of glass by affecting hydration processes, defect stability and crack propagation kinetics.

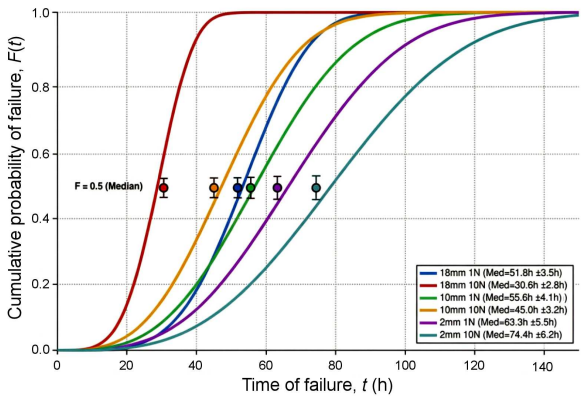

Figure 6. Cumulative probability of failure as a function of load and distance from contact point in water environment

Figure 7 shows a detailed analysis of the results of ring-on-ring bending tests on glass sheets with different loads (1 or 10 N) and distances from the contact point of the lower ring. These tests were done in water, which can change how the material behaves mechanically because of things like hydration, potential corrosion, or interaction with defects caused by indentation. Figure 7 is split into three main parts, each of which gives different information about the mean time to failure.

The first part shows the mean time to failure (MTTF) for different situations. These values were calculated from the experimental failure data and demonstrate clear trends where MTTF decreases with increasing load and increases as the defect distance from the contact point decreases. The results show that the theoretical values of MTTF change a lot depending on the distance and load. In general, the MTTF goes down when the load goes up and rises when the distance from the contact point goes down. The experimental values (Table 1) are generally close to the theoretical values, which demonstrate that the used model is correct. However, the presence of water may have changed these results a little by adding effects related to humidity, such as cracks spreading faster or changes in the properties of the materials in the area.

The second part shows the median fracture strength values for each experimental configuration tested in water. These values are shown as red bars, with the numbers shown directly above each bar. The results demonstrate that median stress values increase as defect distance decreases and vary with applied load. Specifically, at 18 mm distance, the median values are 51.81 MPa (1 N load) and 30.56 MPa (10 N load). At 10 mm distance, median values are 55.57 MPa (1 N) and 45.02 MPa (10 N). At the closest distance of 2 mm, median values reach 63.27 MPa (1 N) and 74.41 MPa (10 N), representing the highest strength values observed. The median values show a similar pattern to the mean times to failure: they go up when the distance from the contact point goes down and decreases when the load goes up. However, the median values are usually lower than the mean times to failure. Because the data is not evenly distributed, the presence of water may have changed these results by speeding up the spread of cracks or changing the properties of the materials in the area.

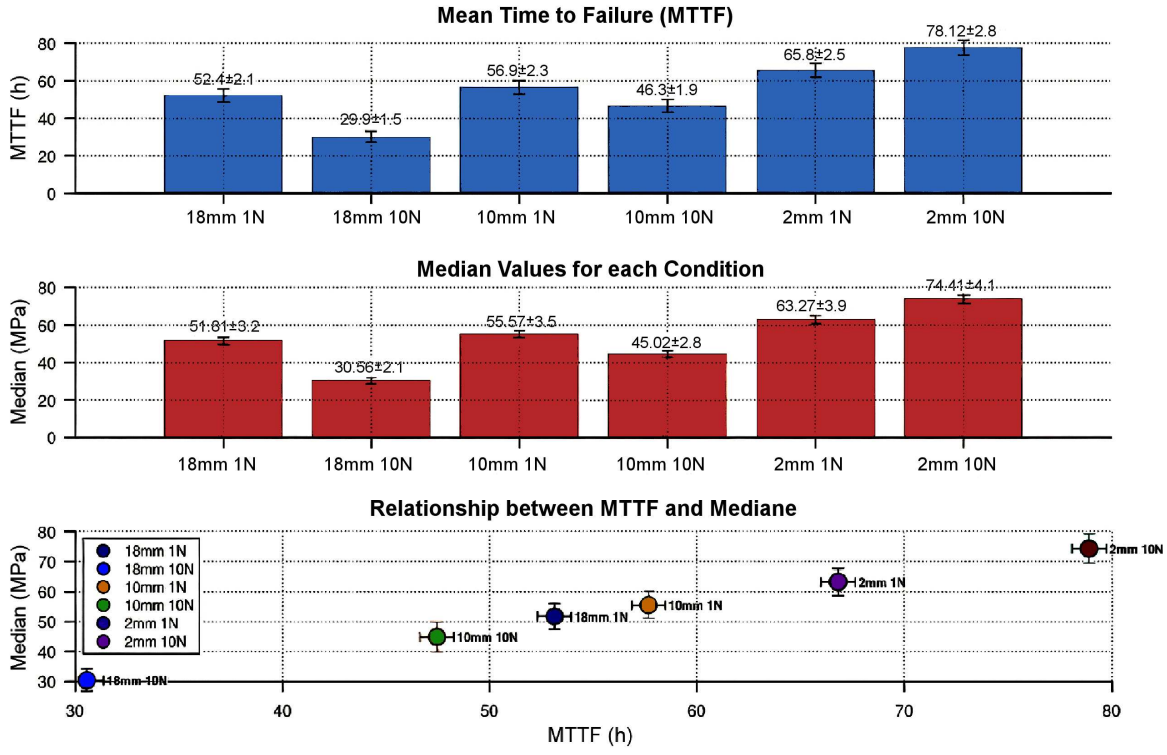

Figure 7. Analysis of mean time to failure (MTTF) and median values for ring-on-ring bending tests under various load and distance conditions

The third section uses a scatter plot to show the connection between MTTF and median values. Each point on the plot stands for a different experimental condition. The results show that there is monotonically increasing relationship between MTTF and median values, but this relationship is not strictly linear. When MTTF goes up, the median values for conditions with 1 N tend to be higher. However, the 10 N condition has a higher median value than expected for its MTTF. This could be because of specific effects related to the higher load and the water, which could make some mechanical weaknesses worse.

Figure 8 shows a comparison between medians that were measured in experiments and those that were calculated using a theoretical model. The different colours on the graph show the different experimental conditions, which are based on diameter (2, 10 and 18 mm) and applied force (1 and 10 N). Trends show that as the diameter gets bigger, the observed and theoretical medians also get bigger. This means that these two variables are positively correlated. The median also changes when the applied force goes up, but this effect is not linear for smaller diameters. For example, with a 2 mm diameter, a higher force (10 N) leads to a lower observed median than a lower force (1 N).

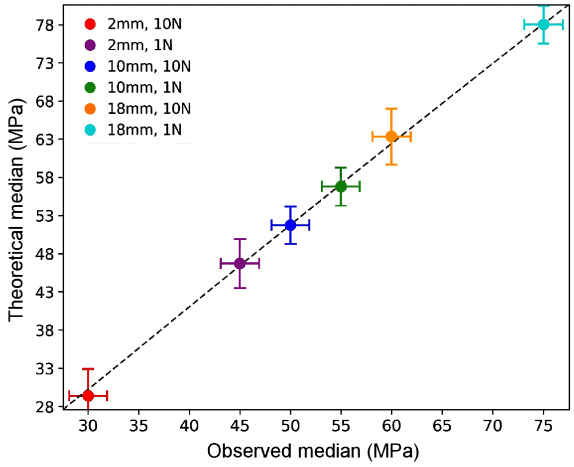

Figure 8. Comparison of observed experimental median values versus theoretical median values predicted by Weibull model, showing linear regression (R^2 = 0.998)

The linear regression line, which has a very high coefficient of determination (R^2 = 0.998), shows that there is a strong relationship between the observed and theoretical values. This shows how accurate the used theoretical model is. The differences between the observed and theoretical medians are usually less than 3 MPa in absolute terms and less than 10% in percentage terms, which shows that the model is reliable.

IV. Discussion

The ring-on-ring (ROR) test is a widely used technique for determining the equi-biaxial strength of glass materials [31]. The tests demonstrated that the severity of the flaws and their location with respect to the loading zone are the two main factors affecting the fracture resistance of float glass submerged in distilled water. Regardless of the distance considered (18 mm, 10 mm, or 2 mm), the results indicate that a higher Vickers indentation load (10 N) produces more critical defects, which results in lower MTTF values when compared to defects created with a lower load (1 N), except for defects located very close to the contact point (2 mm). This is because larger lateral cracks, which serve as potent stress concentrators, are more likely to form under higher indentation loads and accelerate the propagation of defects to failure [32,33].

Defect placement with respect to the zone of maximum stress also has a significant impact. In general, the closer the defect is to this point, the more severe the stress concentration is. However, a notable exception occurs at the 2 mm distance under high load (10 N), where both η and MTTF values are surprisingly elevated despite the proximity to the maximum stress region. This counter-intuitive result can be explained considering several mechanical phenomena.

At very close distances to the contact point, the stress field is highly localized and predominantly compressive on the upper surface, with maximum tensile stress occurring slightly below the surface. Defects located at 2 mm from the centre may be positioned in a region where the tensile stress component is reduced compared to locations at intermediate distances (10 mm), where the stress distribution transitions from predominantly compressive to tensile [34,35].

At such close proximity, multiple stress fields from the indentation defect and the applied load may interact in a complex manner. Under certain geometric configurations, this interaction can result in stress shielding effects that reduce the effective stress intensity factor at the crack tip, thereby increasing the apparent strength [36,37].

The proximity to the loading point imposes geometric constraints that can alter crack propagation paths and reduce crack driving forces. Recent studies on indented ceramics and glasses have shown similar phenomena where defects very close to loading points exhibit enhanced resistance due to the multiaxial stress states that inhibit mode I crack opening [10,11]

Additionally, the β shape factor varies, indicating different statistical stress-rupture distributions, ranging from 4 for defects at 18 mm to 3 for those at 10 mm and 2 mm. This variation in the β factor suggests different levels of defect homogeneity or severity. A higher β value (4) indicates more uniform defect characteristics and less variability in failure stress, while lower β values (3) suggest greater heterogeneity in the defect population and failure mechanisms.

Water in the environment is important because it can affect glass through chemical reactions such as stress corrosion cracking. When tensile stresses are present, water can facilitate microcrack propagation, which

could eventually weaken the material [38]. Water-induced weakening, which varies with stress distribution patterns brought on by load and distance adjustments, is partially responsible for the observed changes in median values.

Higher loads cause cracks to propagate more quickly and increase the likelihood of failure [39,40]. On the other hand, the glass' resistance to failure is influenced by the distance from the contact point in a complex manner [41]. In particular, the median time to failure increases from 53.11 h at 18 mm to 66.80 h at 2 mm at a lower load of 1 N. The median time to failure increases from 30.55 h at 18 mm to 78.91 h at 2 mm at a higher load of 10 N. This illustrates how proximity to the contact point can mitigate the impact of an increased load through the mechanisms described above.

By altering hydration processes, stabilizing flaws, and influencing crack propagation, water can modify the mechanical behaviour of glass. According to studies, crack length and propagation velocity increase with increasing relative humidity [42,43].

The underlying statistical distribution of failure times has a significant impact on the relationship between MTTF (the mean of failure times) and the median (the central value that divides the dataset in half). The relationship between MTTF and the median is constant when these times have an exponential distribution. Significant differences between MTTF and the median, however, may occur when the distribution is skewed, as is frequently the case with reliability data, such as in log-normal or Weibull distributions [44,45]. Since the median is a more robust indicator of central tendency, this phenomenon can be explained by the MTTF's sensitivity to extreme values. A skewed distribution of failure times is thus suggested by the non-linear pattern observed in the correlation between MTTF and median values.

The findings unequivocally demonstrate that raising the applied load generally lowers the median and MTTF, suggesting that increased mechanical stress accelerates the failure process. Increased stress shortens the lifespan of materials by stimulating premature fatigue. Furthermore, local stress concentration is influenced by the distance from the load application point in a complex, non-monotonic manner due to the factors discussed above [46,47].

The rates of crack initiation and propagation determine the mean time to failure (MTTF) of glass materials under aqueous corrosion [48]. The MTTF is reduced by factors that accelerate either of these processes [49]. Shorter MTTF values are associated with higher temperatures, more aggressive chemical environments, and higher stress levels [50]. A power law relationship is frequently used to describe the relationship between stress and MTTF, showing that MTTF decreases exponentially with increasing stress.

The reliability of theoretical Weibull models in forecasting mechanical behaviour under a range of experimental conditions is demonstrated by the study's strong correlation between the observed and theoretical medians ($R^2 = 0.998$). For smaller distances, the observed non-linear mechanical responses (e.g. increase in median values with increased force at 2 mm distance) are consistent with recent findings in fracture mechanics of brittle materials, where stress field redistribution and constraint effects produce distance-dependent and heterogeneous mechanical behaviours [10–12].

V. Conclusions

This investigation explored how Vickers indentation-induced flaws influence the biaxial flexural strength of Mediterranean float glass (MFG), particularly under wet conditions. The researchers used Weibull statistical analysis to model how these micro-defects impact glass reliability. Thirty square MFG samples ($50 \times 50\,mm^2$) were prepared and subjected to two different indentation loads of 1 N (gentle) and 10 N (more severe) at three set distances from the primary loading point (2, 10 and 18 mm). These samples underwent ring-on-ring flexural testing, all while immersed in distilled water, to simulate humid or damp service environments.

Key mechanical parameters such as mean time to failure (MTTF), scale factor (η), shape factor (β) and median failure values were analysed to determine how the size and location of the defects influenced mechanical performance. The findings showed that indentation-induced defects had a pronounced negative impact on the strength of the glass, most notably when those flaws were located near regions of maximum applied stress. Higher indentation loads (10 N) produced more severe flaws, which consistently led to lower MTTF and η values, regardless of their proximity to the load. Defects closer to the loading area also created greater stress concentrations, reducing resistance to fracture. The presence of water further exacerbated these effects by accelerating crack growth and amplifying stress concentration, undermining the structural integrity of the glass.

The Weibull parameters provided insight into the statistical distribution of failure events. β values decreased as defects approached the high-stress zone, indicating increased variability and criticality of flaw-induced fractures. Similarly, η values reflected the compounded influence of defect position and indentation load, highlighting the intrinsic variability of glass strength under different conditions.

Practically speaking, these results underscore the importance of minimizing surface defects especially near high-stress regions when designing float glass for humid environments. The use of Weibull analysis offers a robust, quantitative framework for predicting and optimizing glass performance based on defect characteristics and environmental exposure.

The methodology applied in this research is reproducible and adaptable for other glass types or brittle materials, making it a strong candidate for standard-

ized mechanical testing and quality assurance. Future research could further clarify the mechanisms by which water accelerates crack growth and glass degradation, and also investigate mitigation strategies, like surface treatments or chemical modifications, to enhance resistance to moisture-related damage. These efforts will be critical for developing glass materials suitable for more challenging applications and climates.

References

1. K.R. Tekseth, M.G. Mayani, M. Akram, T. Børvik, D.W. Breiby, "Mapping surface flaws on float glass through Fourier ptychographic quantitative phase imaging", *Appl. Phys. Lett*., **123** (2023) 021108.
2. Y.M. Rodichev, "Surface defects and strength of sheet glass under cyclic and long-term static loading", *Strength Mater*., **47** [2] (2015) 302–313.
3. X. Lian, "Floating glass on-line detection system based on defect feature maximum value method", *IOP Conf. Ser. Earth Environ. Sci*., **242** (2019) 032022.
4. G. Pisano, G. Royer Carfagni, "A micromechanical derivation of the macroscopic strength statistics for pristine or corroded/abraded float glass", *J. Eur. Ceram. Soc*., **37** [13] (2017) 4197–4206.
5. Y. Rodichev, F.A. Veer, "Fracture resistance, surface defects and structural strength of glass", pp. 363–374 in *Challenging Glass 2 – Conference on Architectural and Structural Applications of Glass*, TU Delft, May 2010.
6. M. Kašiarová, T. Rouxel, J.-C. Sanglebœuf, V. Le Houérou, "Fractographic analysis of surface flaws in glass", *Key Eng. Mater*., **290** (2005) 300–303.
7. K.R. Tekseth, M.G. Mayani, M. Akram, T. Børvik, D.W. Breiby, "Influence of single-side ion exchange parameters in LZS and LZSA sintered glass-ceramics", *Bol. Soc. Esp. Ceram. Vidr*., **61** [6] (2022) 663–676.
8. M.A. Cantera, G. Czel, M. Jalalvand, M.R. Wisnom, "Experimental determination of the Weibull parameters in tensile failure using hybrid laminates", *Rev. Mater. Compuestos*, **3** [1] (2019) 47–50.
9. C. Meitao, H. Feng, J. Shi, X. Junlin, Y. Hu, P. Wan, "Low Li_2O content study in Li_2O-Al_2O_3-SiO_2 glass-ceramics", *J. Eur. Ceram. Soc*., **39** [15] (2019) 4988–4995.
10. K. Naumenko, M. Pander, M. Würkner, "Damage patterns in float glass plates: Experiments and peridynamics analysis", *Theor. Appl. Fract. Mech*., **118** (2022) 103264.
11. D. Kinsella, E. Serrano, "Failure modelling of glass plates in biaxial loading: using flaw-size based weakest-link systems", *Glass Struct. Eng.*, **6** (2021) 397–424.
12. A.B. Penurkar, M.K. Samal, A. Syed, J. Chattopadhyay, "Evaluation of strength of float glass using indentation technique and its comparison with results from conventional tests", *Procedia Struct. Integr*., **71** (2025) 150–157.
13. H. He, J.Yu, "Effect of adsorbed water on mechanical and mechanochemical properties of silicate glasses", *J. Non-Cryst. Solids X*, **18** (2023) 100189.
14. U.A. Kini, M. Shettar, S. Suresh, M.C. Gowrishankar, "Effect of different types of water soaking and re-drying on mechanical properties of glass fiber-epoxy composites", *Cogent Eng*., **10** [1] (2023) 2165018.
15. R.E. Hidayati, F.S. Faradilla R. Nurkholifah, R. Nurlina, D. Bayuaji Hartanto, D. Prasetyoko, H. Fansuri, "The effect of water glass source variation on the mechanical properties of fly ash-based geopolymer", *AIP Conf. Proc*., **2339** [1] (2021) 020046.
16. R.M. Richardson, R.M. Dalgliesh, T. Brennan, M.R. Lovell, A.C. Barnes, "A neutron reflection study of the effect of water on the surface of float glass", *J. Non-Cryst. Solids*, **292** [1] (2001) 93–107.
17. M. Tiryakioğlu, "Weibull analysis of mechanical data for castings II: Weibull mixtures and their interpretation", *Metall. Mater. Trans. A*, **46** [1] (2015) 270–280.
18. K.G. Janardan, V.S. Taneja, "Characterization of the Weibull distribution by properties of order statistics", *Biometrical J*., **21** [1] (1979) 1–9.
19. L. Warrington, J.A. Jones, "Perils and pitfalls of Weibull life-data analysis", pp 121–125 in *Ann. Reliab. Maintain. Symp. Proc*., 2005.
20. L.R. Cambrea, D.C. Harris, J.A. Salem, "Weibull analysis and window lifetime prediction: A tutorial", *Proc. SPIE 9453, Window and Dome Technologies and Materials XIV*, 94530A, 2015.
21. M. Tiryakioğlu J. Campbell, "Weibull analysis of mechanical data for castings: A guide to the interpretation of probability plots", *Metall. Mater. Trans. A*, **41** [12] (2010) 3121–3129.
22. T. Li, W.D. Griffiths, J. Chen, "Weibull modulus estimated by the non-linear least squares method: A solution to deviation occurring in traditional Weibull estimation", *Metall. Mater. Trans. A*, **48** (11) (2017) 5516–5528.
23. L.C. Pardini, L.G.B. Manhani, "Influence of the testing gage length on the strength, Young's modulus and Weibull modulus of carbon fibres and glass fibres", *Mater. Res*., **5** [4] (2002) 411–420.
24. K. Trustrum, A.D.S. Jayatilaka, "On estimating the Weibull modulus for a brittle material", *J. Mater. Sci*., **14** [5] (1979) 1080–1084.
25. M., Sorgho, G. Lecomte-Nana, M. Gomina, P. Blanchart, "Microstructure and Weibull distribution of rupture strength of clay-talc ceramics", *Cerâmica*, **65** [374] (2019) 240–245.
26. Q. Zou, J. Wen, "Stress-strength reliability estimation based on probability weighted moments in small sample scenario with three-parameter Weibull distribution", *Reliabi. Eng. System Safety*, **264** [Part A] (2025) 111340.
27. A. Khalili, K. Kromp, "Statistical properties of Weibull estimators", *J. Mater. Sci*., **26** [24] (1991) 6741–6752.
28. V.C. Teles, S.A.G. de Oliveira, W.M. da Silva, "Lateral cracks in soda-lime glass under the threshold load due to the interaction of indentations", *J. Braz. Soc. Mech. Sci. Eng*., **46** (2024) 644.
29. A. Mikowski, F.C. Serbena, C.E. Foerster, C.M. Lepienski, "Statistical analysis of threshold load for radial crack nucleation by Vickers indentation in commercial soda-lime silica glass", *J. Non-Cryst. Solids*, **352** [32-35] (2006) 3544–3549.
30. F. Abdelaziz, "Analyse statistique des défauts de surface générés par sablage du verre sodo calcique", *PhD thesis*, Ferhat Abbas-Sétif University, Algeria, 2010.
31. R. Tandon, B. Paliwal, C. Gibson, "Practical aspects of using Hertzian ring crack initiation to measure surface flaw densities in glasses: Influence of humidity, friction and searched areas", *Philos. Mag*., **93** [21] (2013) 2847–2863.
32. H. He, S.H. Hahn, J. Yu, L. Qian, S.H. Kim, "Factors governing wear of soda lime silicate glass: Insights from comparison between nano- and macro-scale wear", *Tribol. Int*., **171** (2022) 107566.

33. J.E. Ritter, F.M. Mahoney, K. Jakus, "A comparison of Vickers and Knoop indentations in soda-lime glass", pp. 213–223 in *Fracture Mechanics of Ceramics*. Springer USA, 2006.
34. H.-S. Kim, B. Yoo, B.-K. Ha, H.-S. Jeong, S.-H. Park, "Investigation of stress fields for non-standard sized glass plates loaded by ring-on-ring", *J. Eur. Ceram. Soc*., **42** [5] (2022) 2429–2440.
35. Z. Wang, A. Manes, "Stress analysis and fracture simulation of aluminosilicate glass plates under ring-on-ring loading", *Forces Mech*., **5** (2021) 100047.
36. T. Fett, Z. Burghard, A. Zimmermann, F. Aldinger, "Residual stresses and stress intensity factors for Vickers indentation cracks in glass derived from COD measurements", *Adv. Eng. Mater*., **6** (11) (2004) 914–918.
37. G. Qin, Y. Huang, Y. Wang, Y.F. Cheng, "Interaction between corrosion defects with varied orientations on pipelines: A finite element study", *Tunnelling Underground Space Technol*., **136** (2023) 105101.
38. M.J. Meyland, J.H. Nielsen, C. Kocer, "Tensile behaviour of soda-lime-silica glass and the significance of load duration – A literature review", *J. Build. Eng*., **44** (2021) 102966.
39. S. Matsusaka, G. Mizobuchi, H. Hidai, A. Chiba, N. Morita, T. Onuma, "Observation of crack propagation behavior and visualization of internal stress field during wheel scribing of glass sheet", *J. Jpn. Soc. Precis. Eng.*, **81** [3] (2015) 270–275.
40. K. Aoki, S. Matsusaka, H. Hidai, A. Chiba, N. Morita, "High-speed camera observation of crack propagation behavior during wheel scribing of glass sheet", *Proceedings: Conf. Kanto Branch*, 2015.
41. V.M. Sglavo, D.J. Green, "Influence of indentation crack configuration on strength and fatigue behavior of soda-lime silicate glass", *Acta Mater*., **43** [9] (1997) 965–972.
42. S.M. Wiederhorn, "Influence of water vapor on crack propagation in soda-lime glass", *J. Am. Ceram. Soc*., **50** [8] (1967) 407–414.
43. H. Yu, N. Morita, Y. Yoshida, "Study on high quality machining of hard and brittle materials, 2nd Report. Effect of humidity on crack generation and propagation", *Trans. Jpn. Soc. Mech. Eng. C*, **64** [628] (1998) 4410–4415.
44. J.A. Salem, N.N. Nemeth, L.P. Powers, S.R. Choi, "Reliability analysis of uniaxially ground brittle materials", *J. Eng. Gas Turbines Power*, **118** [4] (1996) 863–871.
45. G.D. Quinn, R. Morrell, "Design data for engineering ceramics: a review of the flexure test", *J. Am. Ceram. Soc*., **74** [9] (1991) 2037–2066.
46. Y. Hou, D. Myung, J.K. Park, J. Min, H.R. Lee, A.A. El-Aty, M.G. Lee, "A review of characterization and modelling approaches for sheet metal forming of lightweight metallic materials", *Materials*, **16** [2] (2023) 836.
47. D.J. Green, R. Tandon, V.M. Sglavo, "Crack arrest and multiple cracking in glass through the use of designed residual stress profiles", *Science*, **283** [5406] (1999) 1295–1297.
48. T.A. Michalske, S.W. Freiman, "A molecular interpretation of stress corrosion in silica", *Nature*, **295** [5849] (1982) 511–512.
49. R.J. Charles, "Static fatigue of glass. I", *J. Appl. Phys*., **29** [11] (1958) 1549–1553.
50. S.M. Wiederhorn, L.H. Bolz, "Stress corrosion and static fatigue of glass", *J. Am. Ceram. Soc*., **53** [10] (1970) 543–548.